

This article was downloaded by:

On: 19 January 2011

Access details: *Access Details: Free Access*

Publisher *Taylor & Francis*

Informa Ltd Registered in England and Wales Registered Number: 1072954 Registered office: Mortimer House, 37-41 Mortimer Street, London W1T 3JH, UK



## International Journal of Polymeric Materials

Publication details, including instructions for authors and subscription information:

<http://www.informaworld.com/smpp/title~content=t713647664>

### Intrinsic Differences between Nylon 6 and Nylon 66 Industrial Fibers: Micromechanical and Molecular Analysis

D. C. Prevorsek<sup>a</sup>; H. B. Chin<sup>a</sup>

<sup>a</sup> Allied Signal Inc. Research and Technology, Morristown, N.J.

**To cite this Article** Prevorsek, D. C. and Chin, H. B.(1994) 'Intrinsic Differences between Nylon 6 and Nylon 66 Industrial Fibers: Micromechanical and Molecular Analysis', *International Journal of Polymeric Materials*, 25: 3, 161 – 184

**To link to this Article:** DOI: 10.1080/00914039408029336

**URL:** <http://dx.doi.org/10.1080/00914039408029336>

PLEASE SCROLL DOWN FOR ARTICLE

Full terms and conditions of use: <http://www.informaworld.com/terms-and-conditions-of-access.pdf>

This article may be used for research, teaching and private study purposes. Any substantial or systematic reproduction, re-distribution, re-selling, loan or sub-licensing, systematic supply or distribution in any form to anyone is expressly forbidden.

The publisher does not give any warranty express or implied or make any representation that the contents will be complete or accurate or up to date. The accuracy of any instructions, formulae and drug doses should be independently verified with primary sources. The publisher shall not be liable for any loss, actions, claims, proceedings, demand or costs or damages whatsoever or howsoever caused arising directly or indirectly in connection with or arising out of the use of this material.

# Intrinsic Differences between Nylon 6 and Nylon 66 Industrial Fibers: Micromechanical and Molecular Analysis

D. C. PREVORSEK and H. B. CHIN

*AlliedSignal Inc. Research and Technology, Morristown N.J. 07962-1021*

*(Received September 20, 1993)*

In airdrop applications we noted significant performance advantages of nylon 6 over nylon 66. These advantages are noted in bending fatigue, abrasion resistance and retention of properties on repeated use. To explain this advantageous behavior of nylon 6 we carried out comprehensive morphological and micromechanical analyses. These in turn, provided a better understanding of the role of subtle structural differences between nylon 6 and nylon 66 in the performance of fabrics used in parachutes.

The study showed that the outstanding bending fatigue resistance and retention of properties of nylon 6 on repeated use must be attributed to a much narrower distribution of long period, anti-parallel arrangement of molecules in the alpha crystalline form, and the existence of gamma crystalline form which is energetically close to the alpha form with shorter repeating unit.

**KEY WORDS** Nylon 6, nylon 66, fabric mechanics, bending fatigue, abrasion resistance

## 1. INTRODUCTION

Variations in draw ratio, heat treatments, thermal contraction, etc. coupled with minor chemical modifications produce large property changes in polymeric fibers such as nylon 6 and nylon 66. These treatments are technologically exploited to tailor properties for specific applications. Because of this ability to alter the properties through the manipulations of morphology, both representatives of the aliphatic polyamides are used in a variety of applications.

It is therefore surprising that despite this ability to control and vary the morphology, we are very seldom able to develop a product based on nylon 6, which is equivalent in performance to nylon 66 product, for the application where nylon 66 is used. Sometimes these intrinsic and uncorrectable differences are favorable to nylon 66, sometimes to nylon 6.

The glass transition temperature of nylon 6 and nylon 66 is the same, therefore the two polymers share almost all markets from the apparel, lingerie, carpet yarns, narrow fabrics to tire cords, etc. The differences in behavior and performance we see in all these applications are associated mainly with the higher melting point, higher degree of crystallinity and faster rate of crystallization of nylon 66. These

polymer characteristics are responsible for the well publicized and commercially exploited advantages of nylon 66 such as; higher modulus, better dimensional stability under load, better stability and crimp retention, lower moisture sensitivity, lower flat-spotting, better retention of properties on fabrication at elevated temperature (cured strength loss) etc.

Lately we were investigating the potential of using nylon 6 fibers for parachute components where the fabrics are exposed simultaneously to a variety of types of deformation. These are tensile impact, bending, abrasion and cyclic loads. Under cumulative effect of these four fundamental types of deformation, nylon 6 outperformed the currently qualified nylon 66 product by a wide margin. To explain this remarkable advantage of nylon 6 for this application we have undertaken a fundamental study, interpreting the observed results in terms of molecular and morphological characteristics of these two fibers.

## 2. RELEVANT MORPHOLOGICAL DIFFERENCES BETWEEN NYLON 6 AND NYLON 66

It will be shown that observed intrinsic property differences are caused by subtle morphological differences between the two fibers relative to:

- Unit cell characteristics
- Long period characteristics
- Critical crystallographic structure

It is important to note that these subtle morphological differences are at this time technologically, scientifically as well as conceptually uneliminatable.

### A. Unit Cell Characteristics

Small-Angle X-ray Scattering (SAXS) patterns of nylon 6 show only the  $\alpha$  form and can be indexed on a monoclinic unit cell with the following dimensions<sup>1</sup> (Figure 1):

$$a = 9.59 \text{ \AA}$$

$$b = 17.23 \text{ \AA (chain axis)}$$

$$c = 8.15 \text{ \AA}$$

$$\beta = 66.6^\circ$$

These values agree with those quoted in the literature ( $a = 9.56 \text{ \AA}$ ,  $b = 17.2 \text{ \AA}$ ,  $c = 8.01 \text{ \AA}$ ,  $\beta = 67.5^\circ$ ). We found little differences in these cell dimensions from one fiber to another. The crystalline index for all the nylon 6 fibers are  $\sim 67\%$ .

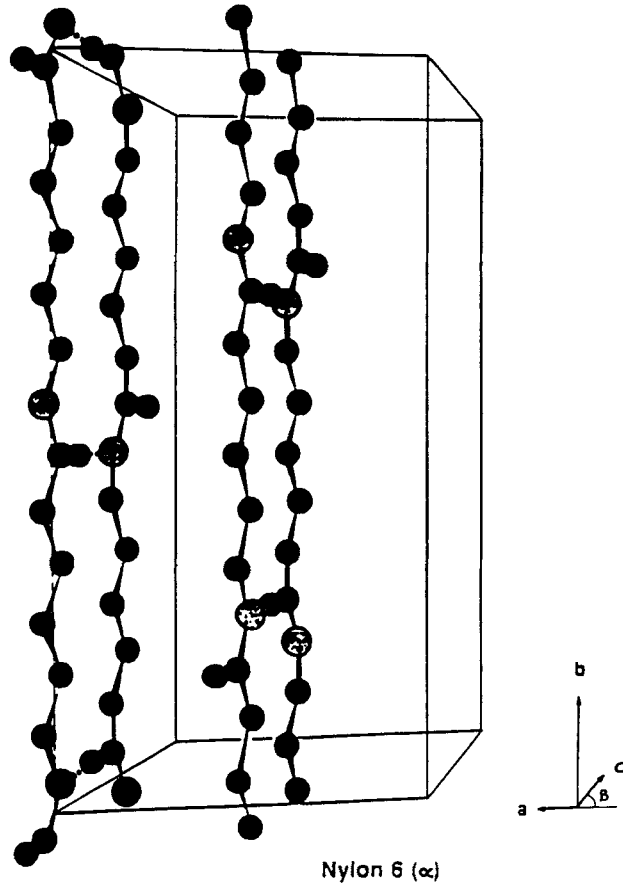


FIGURE 1 Crystal structure of nylon 6.

Within our estimated error of  $\pm 2\%$  we find no differences in the crystallinities of these fibers.

The nylon 66 patterns were indexed on a triclinic unit cell ( $\alpha$  form) and the following dimensions were obtained (Figure 2):

$$a = 4.99 \text{ \AA}$$

$$b = 5.51 \text{ \AA}$$

$$c = 17.22 \text{ \AA (chain axis)}$$

$$\alpha = 50^\circ, \quad \beta = 77^\circ, \quad \gamma = 62^\circ$$

Typical values quoted in the literature are:  $a = 4.9 \text{ \AA}$ ,  $b = 5.4 \text{ \AA}$ ,  $c = 17.2 \text{ \AA}$ ,  $\alpha = 48.5^\circ$ ,  $\beta = 77^\circ$ , and  $\gamma = 63.5^\circ$ . The crystallinity of nylon 66 is  $\sim 70\%$  and thus slightly higher than that for nylon 6.

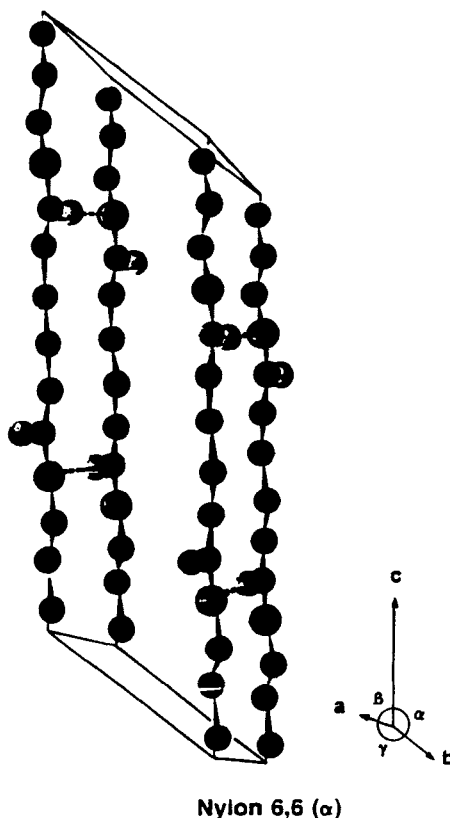


FIGURE 2 Crystal structure of nylon 66.

### B. Long Period Characteristics

Another important difference between the structure of the two fibers is the lamellar spacing obtained from SAXS pattern. The periodicity along the microfibrils (long period) is  $\approx 91 \text{ \AA}$  for nylon 66 and  $86 \text{ \AA}$  for nylon 6.

The standard deviation  $\sigma$  for the nylon fibers calculated from seven different fibers is  $1.5 \text{ \AA}$ . Thus the difference of  $\sim 5 \text{ \AA}$  is more than  $3\sigma$  and, therefore, is significant and cannot be attributed to experimental errors. In addition, the corresponding reflection is much sharper in all but one nylon 6 fiber (Full Width at Half Maximum, FWHM  $\sim 0.1^\circ$ ) than in nylon 66 (FWHM  $\sim 0.37^\circ$ ). This suggests a much narrower distribution about the mean spacing in nylon 6 than in nylon 66.

In quantitative terms, the width of the long period distribution of the two fibers for industrial applications, e.g., tire cords, can be compared using the coherence length  $l_{\text{coh}}$  estimated by the Sherrer equation<sup>2</sup>:

$$l_{\text{coh}} = \lambda / [\Delta(2\theta)\cos \theta] \quad (1)$$

where  $\lambda$  = wavelength (1.543 Å),  $2\theta$  = scattering angle, and  $\Delta(2\theta)$  = full width at half-maximum. These estimates lead to:

$$l_{\text{coh}} (\text{nylon 6}) \approx 800 \text{ \AA}$$

$$l_{\text{coh}} (\text{nylon 66}) \approx 250 \text{ \AA}$$

This difference is also significant and reflects a much sharper periodicity in crystalline dimensions along the microfibrils in nylon 6 than in nylon 66 fibers.

The key fiber characteristics we will use in our analysis are listed in Table I. For the discussion below, it is important to note that an extended chain nylon 66 molecule is directionally symmetrical. That means that the atomic sequence is the same regardless whether we move up or down the chain. With nylon 6, on the other hand, the atomic sequence in one direction differs from that in the opposite direction.

### 3. MICROMECHANICAL INTERPRETATION OF BENDING FATIGUE

An experimental evidence that illustrates well the inherent advantages of nylon 6 under severe bending and/or repeated use under complex loadings (such as in parachute components) is the loss of filament strength after biaxial flexural fatigue. The large performance difference between the two types of fibers is shown in Figure 3.

We were able to explain these differences in flexural fatigue using a micromechanical analysis of the microfibrillar structure (Figure 4) of nylon 6 and nylon 66 fibers shown in Tables I and II. We found that the lower microfibril modulus and the shorter and much more regular longitudinal periodicity (long period) are the key factors in bending fatigue resistance. We were particularly interested in the shorter nylon 6 crystallite dimension (crystal length) in the fiber direction, and much smaller scatter of the long period about the mean-length. Both factors are favorable for the mechanical properties affecting the performance of parachute fabrics. (See Section 7)

Our hypothesis is that the differences in the crystal length, degree of crystallinity, rate of crystallization and the heat of fusion reflect the differences in the structure of the two polymer chains.

To explain the differences in the crystal length, we must consider two factors; the heat of fusion and the strain of molecules in the amorphous phase. This strain develops upon formation and growth of crystallites. The growth of the crystallites stops when the increment in the heat of fusion associated with the incremental growth in crystal length equals the increment in the strain energy of the amorphous molecules associated with the corresponding increase in crystallite length. In our calculations, we show that, with the crystallites that contain the molecules in anti-parallel arrangement, the strain of the amorphous molecules is significantly larger than with the crystallites where the molecules are directionally symmetrical.

The calculations assume that initially both nylon 6 and nylon 66 crystallize into

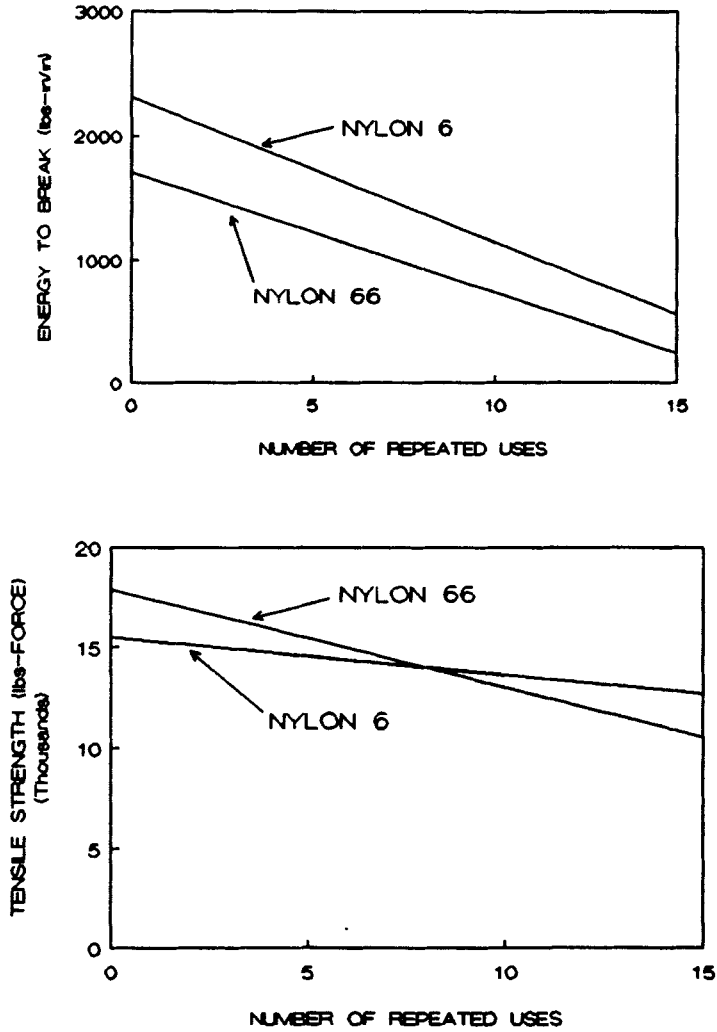


FIGURE 3 Performance of nylon 6 and nylon 66 under repeated use. (Airdrop simulation by tensile impact over sharp edge).

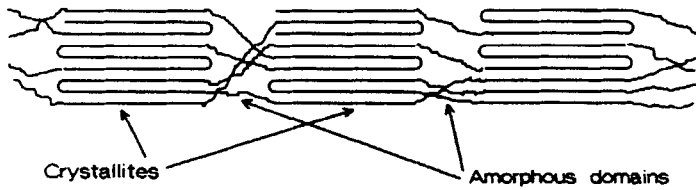


FIGURE 4 Schematic model of microfibril in nylon 6 and nylon 66 fibers.

TABLE I  
Fiber characteristics affecting the crystal length distribution

	Nylon 6	Nylon 66
Degree of crystallinity (%)	67.0	70.0
Specific heat of fusion (J/g)	58.0	64.0
Crystal length (Å)	57.6	61.0
Crystal size distribution	narrow	wide
Crystallization rate coeff.	63.0	83.0
Type of crystallinity chain direction in crystal	anti-parallel	parallel

TABLE II  
Crystallographic data

	Degree of crystallinity, %	Amorphous orientation (Integral breadth in degrees of the azimuthal intensity distribution)	Long period, Å	Size of amorphous domain, Å
Nylon 6	67	30	86	28.7
Nylon 66	70	36	91	30.3

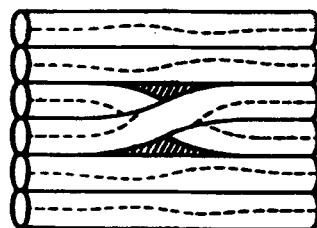
a crystal lattice where the chain direction is random. This means that the nylon 6 crystallization proceeds through an aggregation of a random mixture of parallel and anti-parallel molecules. This leads to the formation of a mixed crystal involving both  $\alpha$  and  $\gamma$  domains. This randomly formed crystal is then transformed into an  $\alpha$  crystal through the molecular rearrangements involving the motion of disclinations through the crystal as it is shown schematically in Figure 5. Based on the calculations by assuming initially an arbitrary arrangement of molecules in a crystalline layer and by transforming this randomly constructed layer into a layer of  $\alpha$  crystal of the same length, we were able to estimate the increment in the strain of the amorphous molecules adjacent to the crystal. The calculations show that with the anti-parallel crystals (such as  $\alpha$  form of nylon 6) the strain on the amorphous molecules is significantly higher than with non-directional chains such as nylon 66. This anti-parallel arrangement of polymer chains in the  $\alpha$  crystal of nylon 6 and its lower heat of fusion are then the two main factors responsible for the shorter crystallite length in nylon 6 than with nylon 66. (See Appendix)

#### 4. FACTORS CONTROLLING THE WIDTH OF LONG PERIOD DISTRIBUTION

The long period distribution is, according to the finite element analysis of microfibril bending, a key factor affecting bending fatigue in addition to the long period length. A broad distribution of long period (irregular long period) gives rise to a large variation in the ratio of amorphous domain to crystalline domain length ( $l_a/l_c$ ) which is sensitive to the stress level in the microfibrils under bending (see Figure 13).



## Disclination phenomenon of polymer chains



REARRANGEMENT OF 'RANDOM' CRYSTAL  
TO  $\uparrow\downarrow$   $\alpha$  CRYSTAL IN NYLON 6

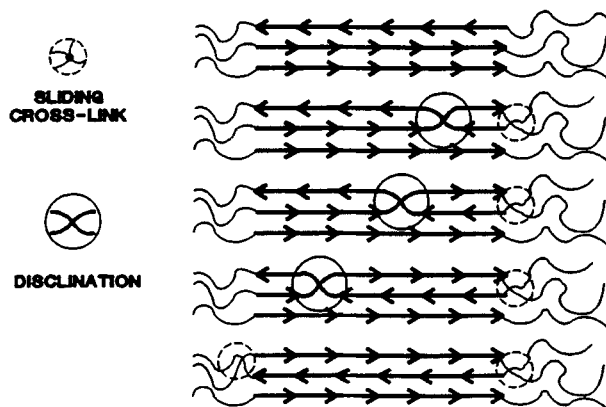


FIGURE 5 Rearrangement of molecular chains in a crystalline layer.

The results can be illustrated considering the bending or subjecting the ensembles of microfibrils held together fairly strongly by the interfibrillar tie molecules to stress perpendicular to the fiber axis. It is obvious that large differences in the long period of adjacent microfibrils will lead to large strain gradients, hence large stress gradients, on bending as well as weakening of transverse properties. In this respect, it is important to note that there exists surprisingly large difference in the regularity of the long period between nylon 6 and nylon 66. As mentioned earlier, a measure of its distribution is the coherent length estimated by the Sherrer equation which amounts to 800 Å for nylon 6 and 250 Å for nylon 66. Figure 6 represents the situations of a very uniform distribution, (a), of long period (nylon 6) and non-uniform distribution, (b) (nylon 66).

The experimental observation that the fluctuation about the average long period in nylon 6 is much smaller than in nylon 66 has been recorded many times<sup>1</sup> (see Figure 7). But so far, this result caused little interest because its relevance in mechanical properties was not understood. After determining the importance of the effect of the long period distribution on bending fatigue and transverse properties (fibrillation) under severe bending, etc., we became immediately interested in establishing the molecular characteristics causing this remarkable difference in the macrolattice characteristics of the two fibers. A successful analysis of this

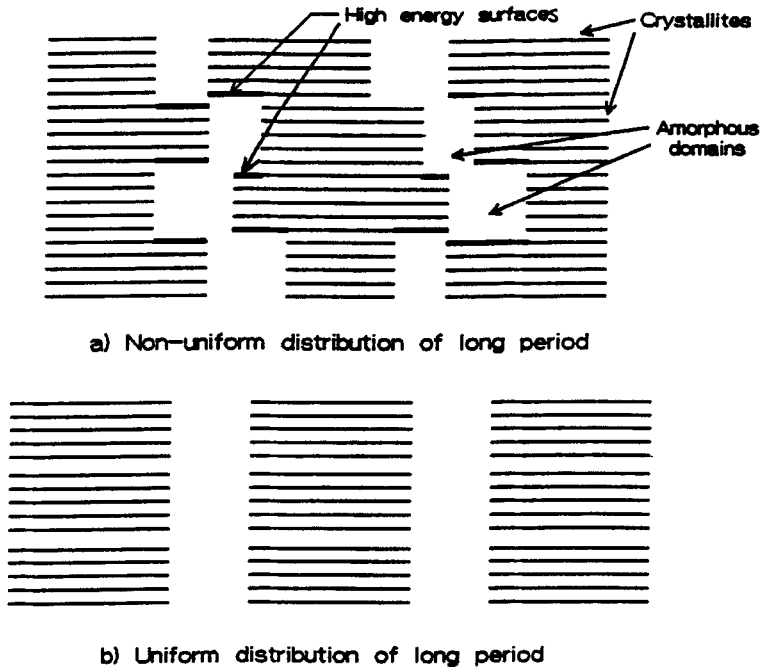


FIGURE 6 Macrolattice structure of crystallites of nylons.

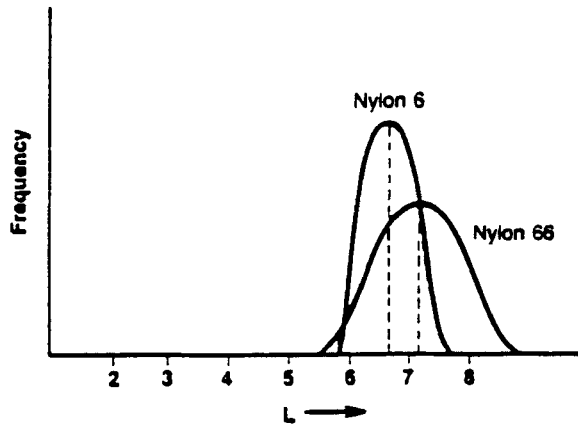


FIGURE 7 Schematic of long period distribution in nylon 6 and nylon 66.

problem would not only provide an explanation for the inherent difference in durability between nylon 6 and nylon 66 but also provide valuable guideline for future polymer research and molecular design.

Our analysis shows that the variation in the width of the long period distribution is caused by the several factors; crystallization rate, the cohesive energy of the system as it is reflected in the heat of fusion of the crystalline phase and the length of crystal lattice dimensions along the fiber direction, which is also fibril direction, and b-axis crystallite direction. While the crystal lattice dimensions of nylon 6 (b-

axis in Figure 1) and nylon 66 (c-axis in Figure 2) are almost equal (17.23 vs. 17.22 Å), the repeating unit of polymer chain of nylon 6 is only one half of that in polyhexamethylene adipamide (nylon 66). Further discussion on the non-uniformity of long period length is given below (Section 5).

Since it has been shown that the crystallites of adjacent microfibrils are strongly held together by epitaxial crystallization of extended interfibrillar molecule,<sup>3</sup> it can be inferred that large mismatched crystal areas in Figure 6a lead to the weakening of the structure. These effects should be particularly noticeable in cases of shear, bending and straining in the direction of the fiber axis.

## 5. FACTORS CONTRIBUTING TO THE NON-UNIFORM LONG PERIOD

### A. Isolated Microfibril

If we assume that the nylon 6 and nylon 66 melts and molten filament extrudates are of very similar structure and homogeneous, then the variations in crystallite dimensions must be attributed primarily to local fluctuations in temperature. These local temperatures are not only the result of heat transfer from the heating medium and heat exchange with the environment but are also affected by the heat effect associated with the viscous flow of drawing and crystallization exotherm. In a process where the external heat transfer effects are maintained constant for both fibers, we must then be concerned primarily with the heats of crystallization and the change in the crystallization rate as function of temperature. The respective heats of crystallization of nylon 6 and nylon 66 amount to 57.59 J/g and 64.19 J/g.

In regard to the coefficient of the crystallization rate, the work of Y. P. Khanna<sup>4</sup> is noteworthy. Khanna established that the crystallization rate coefficient of nylon 66 is about 25% higher than that of nylon 6. The sensitivity to temperature changes combined with a higher heat of crystallization of nylon 66 are in our opinion the source for the observed nonuniformity in crystallite dimensions in nylon 66 fibers which we believe is responsible for its poor flexural fatigue and excessive loss of properties on repeated exposure to the complex loading histories.

### B. Macrolattice-Ensemble of Microfibrils

Consider now the mismatched macrolattice (Figure 6). Since it has been established that the adjacent crystals in the lattice are strongly bonded, it follows that; a) the mismatched areas of crystals facing the amorphous domains must have a higher surface energy than the crystal surfaces facing another crystal, and b) the mismatched macrolattice (Figure 6a) is also much weaker in transverse direction than the regular structure (Figure 6b).

Since the macrolattice structure shown in Figure 6a is energetically less favorable than more regular structure (Figure 6b), there will be a tendency to convert (a) into (b) provided such transformation conditions exist, thus, sharpening of LP (long period) scatter or development of uniform macrolattice has been observed on heating and relaxing of fibers. Therefore, it is quite clear that such processes take place in the manufacture of fibers. The energetics of this process are discussed.

It is well known that under stress and/or heating, polymers undergo solid state transformation through the motions of chain imperfections (dislocations, etc.) through the crystal. Consider now once more the situation of mismatched long period in Figure 6. Since the internal energy of the system (Figure 6a) is higher due to additional surface areas, the system would show a tendency of rearrange and assume the lower energy structure shown in Figure 6b.

The driving force  $f$  for flow change (solid state transformation) is associated with the increments of internal energy associated with the high energy surfaces of crystals,  $A_{c-a}$ , that are adjacent to amorphous domain, i.e.,

$$f = KA_{c-a}E_{sca} \quad (2)$$

where  $E_{sca}$  is the specific surface energy and  $K$  is a constant.

Assuming that the chain moves from one crystal to the other by the motion defects, then the force resisting this motion is proportional to the excess free energy associated with the formation of the defect and the distance the chain has to move from one equilibrium position to another. To facilitate the discussion we will refer to this quantity as the "jump distance."

The energy, associated with the formation of defects that can move through the crystal lattice and lead to the longitudinal displacement of molecule, depends on the characteristics of the polymer chain and the chain interactions in the polymer crystal. Within the scope of this discussion, we can assume that the main chain characteristics of nylon 6 and nylon 66 (atomic groups, rotational barriers, etc.) are equal. That means that we consider the conformation energetics of isolated molecules of these two polymers being equal. In other words, we assume the energies associated with the conformational changes (kinks, loops twists, etc.), which are part of a defect that travels through the crystal, to be equal for both polymers.

The energies associated with the expansion of the crystal which are necessary to accommodate various defects are however larger in nylon 66 than in nylon 6. This conclusion is based on the heat of fusion of these two polymers.

There is however another factor that should be considered in the energetics of solid state rearrangements of the molecules in the crystalline phases of nylon 6 and nylon 66, i.e., the length of the repeating unit, which is twice as long in nylon 66 than in nylon 6. While the exact crystal rearrangement is achieved only by a longitudinal displacement of nylon 6 molecule by the full length of the unit cell dimension in the polymer chain direction, a somewhat less energetically favorable modification is also possible when the chain is displaced by one repeating unit of the polymer chain or one half the distance of crystal lattice dimension (in its  $b$  axis direction), provided the chain is twisted by about  $120^\circ$ . This longitudinal displacement combined with the  $120^\circ$  twisting leads to the  $\gamma$  form of the nylon 6 crystal. This crystal form is quite stable and melts only  $6^\circ\text{C}$  to  $8^\circ\text{C}$  lower than the more stable crystalline form.

We propose that the solid state crystalline rearrangement in nylon 6 proceeds by longitudinal displacement involving jump distance which are only one half of the jump distance in nylon 66 and the twisting of the repeat unit to alternately

form  $\alpha$  and  $\gamma$  crystalline forms. In the absence of quantitative crystal lattice and chain conformation analyses, we will use the melting point difference to estimate the energy differences between the  $\alpha$  and  $\gamma$  crystals of nylon 6. Assuming that the entropy difference on melting is about the same for the two polymers, it follows from the melting point difference of  $\alpha$  and  $\gamma$  modification (220 vs. 216°C) and the known specific heat of fusion of the  $\alpha$  crystalline form (58 J/g) that the heat of fusion of the  $\gamma$  modification of nylon 6 is only about 3% lower than that of the  $\alpha$  modification. This can be shown by the following equations:

$$T_m = \frac{\Delta H}{\Delta S} \quad (3)$$

and

$$\frac{\Delta H_\alpha}{T_{m\alpha}} = \frac{\Delta H_\gamma}{T_{m\gamma}} \quad (4)$$

where  $T_m$  and  $\Delta H$  are the melting point and heat of fusion, and the subscripts  $\alpha$  and  $\gamma$  denote the  $\alpha$  and  $\gamma$  crystal modifications, respectively. The process of moving the polymer chain from one crystal to another continues until the drag on the molecule (resistance to move) matches the driving force. The critical (equilibrium) surface area of crystals,  $A_{c-a}$ , at which the process stops, can be approximated by

$$A_{c-a} \approx K_s \Delta H \cdot L \quad (5)$$

where  $L$  is the jump distance and  $K_s$  is a constant.

As shown above, since the difference in heat of fusion between the  $\alpha$  and  $\gamma$  crystals is small and the jump distance is the same, the critical surface area of crystals ( $A_{c-a}$ ) is virtually equal in both the crystal phases. This implies that the long period distribution in the  $\alpha$  and  $\gamma$  crystals in nylon 6 is almost the same. However, both heat of fusion and jump distance of nylon 66 are higher than those of nylon 6. Consequently,

$$A_{c-a}(\text{nylon 66}) \gg A_{c-a}(\text{nylon 6}) \quad (6)$$

Thus, the differences in heat of fusion and the jump distance explain the large difference in the long period distribution between the two polymers.

It should be noted that, in the conversion of the  $\alpha$  configuration into the less stable  $\gamma$  configuration, the system will consume about 3% of the strain and/or thermal energy, but some of these lost energy will be however recovered because the resistance to the motion of the dislocation and/or lateral displacement of the molecule will be lower in the less stable  $\gamma$  form.

In summary, we attribute the ease of longitudinal displacement of molecules in nylon 6 in comparison to nylon 66 to the following factors; lower energy to accommodate crystal defects associated with chain conformations involved in the longitudinal displacements for the molecule, shorter repeating unit allowing a 50%

reduction in the jump distance from one equilibrium position to another, and the existence of a stable and energetically very similar  $\gamma$  modification that involves only a  $120^\circ$  twist in the polymer chain.

The ease with which solid state crystalline rearrangements take place in nylon 6 is a key factor contributing to its outstanding bending and torsional fatigue resistance and impact resistance. The ease of solid state rearrangement is responsible also for the uniform long period distribution and short crystal length in nylon 6. On the other hand, the same phenomena are responsible for poor dimensional stability, higher cured strength loss and high shrinkage at elevated temperatures of nylon 6 relative to nylon 66.

To verify this conclusion we examined the changes in the morphology of nylon 6 and nylon 66 fibers subjected to fatigue. The Wide Angle X-ray Diffraction (WAXD) data show that decrease in the crystalline order, as measured by an Index of Crystalline Perfection (ICP), in nylon 6 is 3 times larger than in nylon 66 (from  $3.31^\circ$  to  $3.247^\circ$  i.e., by  $0.084^\circ$  in nylon 6 from  $3.013^\circ$  to  $2.985^\circ$  i.e., by  $0.028^\circ$  in nylon 66).

This clearly shows that under stress, the crystallites in nylon 6 undergo much larger changes in crystalline order than the crystallites in nylon 66. While their overall dimensions remain about the same as indicated by the SAXS data. We believe that through these solids state transformation of nylon 6 crystals, the molecular strain in the amorphous domain is relieved and thus the chain scission and crack formation is retarded.

In nylon 66, on the other hand, the crystals act more like an inert particulate reinforcement with very sharp boundaries and very limited capabilities to release molecular stress through solid state rearrange.

## 6. ANALYSIS OF LOSS PEAK

Additional consequences of long period distribution are reflected in the shape of the loss peak of conditioned tire codes. The mechanical-loss-temperature curves of well conditioned nylon 6 and nylon 66 tire cords at 1% strain amplitude are shown in Figure 8a. Comparing the two curves, we recognize the following differences:

- a. The maximum mechanical loss (loss peak) is higher with nylon 6 than with nylon 66.
- b. The temperature of the peak loss is higher with nylon 66 than with nylon 6.
- c. The slope of the mechanical-loss-temperature curve before and after the peak loss temperature is steeper with nylon 6 than with nylon 66 cord, i.e., the curve for nylon 6 falls off faster than for that of nylon 66.

These features are the source of the observed difference in tire performance which we have analyzed and explained as follows:

- a. The difference in the maximum loss 2.35 and 2.15 mJ/cm/sec for nylon 6 and nylon 66 respectively should be attributed to higher crystallinity of nylon 66 fiber.

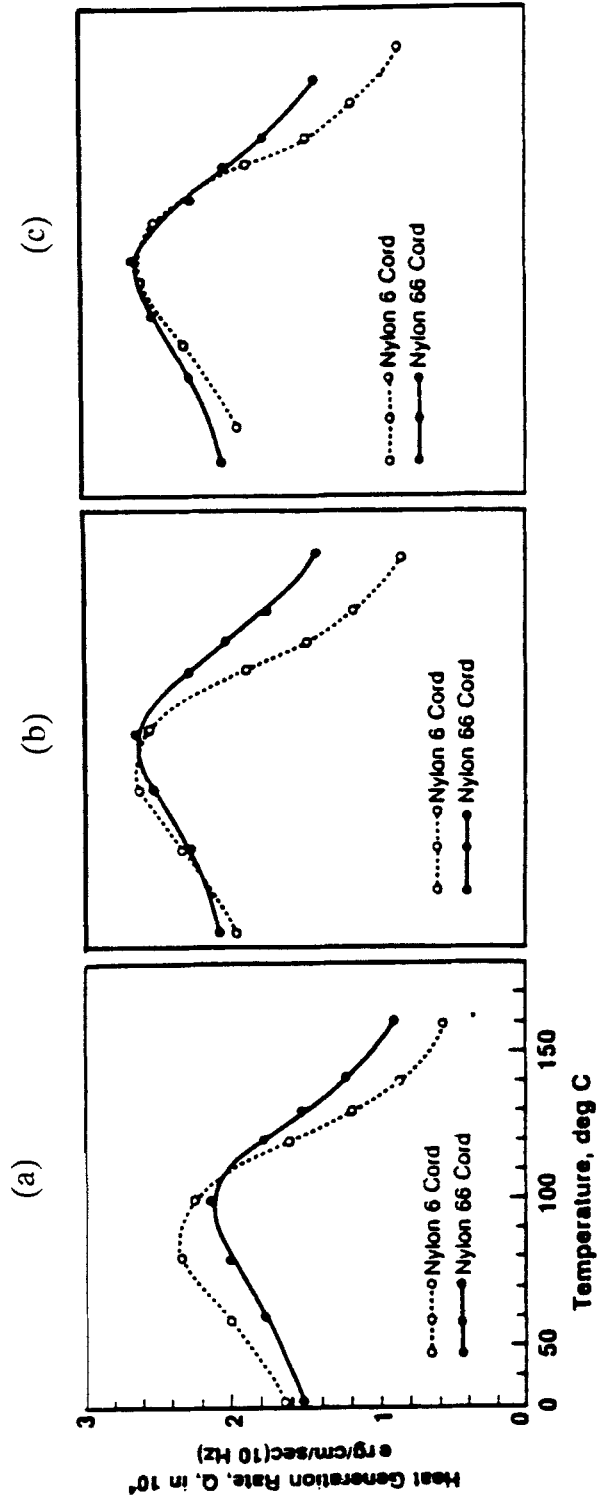


FIGURE 8 Mechanical loss vs. temperature curves of nylon 6 and nylon 66 cords: (a) Experimental measurements; (b) Vertical adjustment to account for differences in degree of crystallinity; (c) Vertical and horizontal adjustments to compare the slopes of curves before and after the temperature at the peak of loss.

- b. After vertical shift to account for this effect (see Figure 8b), the two curves do not overlap, but the peak temperature of nylon 66 is at about 10°C higher than that of nylon 6. This should be attributed to the higher melting point of nylon 66. However, the difference of 10°C is much less than that reported for unoriented polymers (25°C) and also less than that of unconditioned fibers (13°C).

The difference in  $T_g$  between the unoriented polymers and mechanically conditioned tire cords is an interesting and a technologically very important finding. The key observation is that the corresponding shifts in loss peak temperatures equal 48°C for nylon 6 and only 34° for nylon 66 in spite of the slightly higher degree of crystallinity in the latter (Table II). This shows that the orientation and condition produce much larger tightening effects on the mobility of the amorphous domains in nylon 6 than in nylon 66 fibers.

Two structural characteristics contribute to this effect, the amorphous orientation function and the long periods (Table II). Since the amorphous domain in nylon 6 is shorter than in nylon 66, the amorphous molecules are under more severe constraint than those in longer domain in nylon 66. The same trend is expected from values of amorphous orientation function for two types of fibers.

- c. When the second effect is also taken into consideration and the curves shift horizontally to superimpose the maxima of the two loss factor peaks, we come to the situation presented in Figure 8c. After accounting for the differences in degree of crystallinity, melting point, amorphous orientation, and the size of the amorphous domains by vertical and horizontal shifting of the two dispersion peaks, we see that the loss peak of nylon 6 is narrower than that of nylon 66. This indicates a narrower distribution of relaxation time in nylon 6, which in turn reflects a narrower distribution in structure (orientation, size, packing, etc.) of the amorphous domains. Regardless of the cause, it is clear that the amorphous domains in nylon 6 are much more uniform than in nylon 66.

This was a most interesting finding and we were concerned that it may be rather difficult to explain in terms of morphological characteristics of fibers. It requires an independent determination of the distribution of structure of amorphous domains, and there is no precedent in the literature correlating the morphological data of fibers with the width of the relaxation times. We hoped that some information regarding this characteristic of fiber morphology can be obtained by analyzing the SAXS pattern of the two fibers. The angle of the meridional reflection indicates the spacing between the lamellae in the microfibrils. The long period  $L$  is the sum of the length of crystalline ( $l_c$ ) and amorphous ( $l_a$ ) domains (Figure 9). As noted before,  $L$  (nylon 6) = 86 Å and  $L$  (nylon 66) = 91 Å. It is also well known that  $l_a \approx \frac{1}{3}L$  and therefore, variations in  $L$  also indicated changes in  $l_a$ .

From the width of meridional reflection corresponding to the periodicity of amorphous and crystalline domains in the microfibrils, we can determine the distribution of the length of the long period  $L$  and, indirectly, that of the length of the amorphous domains ( $l_a$ ). In Figure 10 are shown the SAXS meridional scans of the two fibers. Since the reflection of nylon 66 is much wider than that of nylon



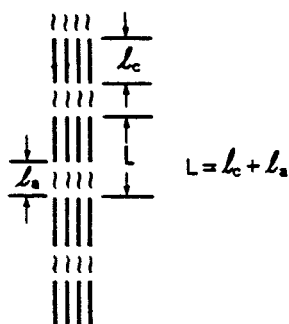


FIGURE 9 Schematic representation of crystalline lamellae ( $l_c$ ) and interlamellar amorphous region ( $l_a$ ).  $L$  is the long period from SAXS measurement.

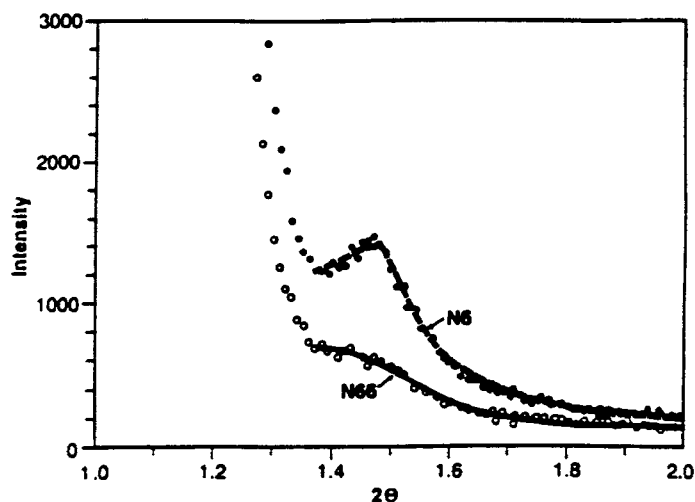


FIGURE 10 Small-angle x-ray scattering curves of nylon 6 and nylon 66 fibers.

6, we can infer that the variations in crystalline and amorphous domain length are much larger in nylon 66 than in nylon 6 (Figure 7). This, in turn, should give rise to a wider distribution of relaxation times in nylon 6. The shape and position of loss peak is particularly important in tire performance analysis.

When the role of tire cord in tire temperature rise was first reported and the differences in performance of nylon 6 vs. nylon 66 reproduced in various laboratories, we anticipated that systematic cord manufacturing research would ultimately lead to tire cords with greatly improved heat generation characteristics. The possibility was also expressed that the differences between nylon 6 and nylon 66 could be eliminated or, at least greatly reduced.

On the basis of several years of research and data available to date, it is clear that the control of fiber and cord morphology and viscoelastic properties through fiber and cord manufacturing procedure has its limitations. The differences in greige and dipped, tensilized cords introduced through process variables may be quite significant. However, these differences appear to be unstable, and they gradually diminish and disappear under thermomechanical conditioning, which the cords

experience in tires during service. Consequently, the nylon 6 and nylon 66 cords removed from the tires after service can always be identified without difficulties by viscoelastic behavior described and used in this study. This trend has now been confirmed with parachute sling samples produced by Murrdoch and Elizabeth Webbing.

**7. BENDING BEHAVIOR OF FIBRILS OF NYLON FIBERS**

The properties of nylon fibers depend on their morphological structure. The elemental building blocks of nylon fibers are microfibrils consisted of crystalline lamellae (crystallites) and disordered amorphous domains (Figure 4).

The structure of the crystallites and amorphous domains in the microfibrils is the major factor affecting the behavior of the nylon fibers. The major parameters involved in the morphological structure of microfibrils include the long period, ratio of length of crystallite to amorphous domain, and ratio of moduli of crystallite to amorphous domain.

To study the effects of these morphological parameters on the stress and strain levels developed in the fiber under load such as bending, a micromechanical analysis was performed using the finite element analysis technique.<sup>5,6</sup> A single microfibril having the dimension of 909 Å long and 70 Å in diameter was modeled as a cylinder as shown in Figure 11. The microfibril was then subjected to a bending load, i.e., both ends were held fixed in vertical direction and the middle was pushed upward 160 Å.

The properties (moduli) of the crystallites and amorphous domains used are shown in Table III, in which X coordinate is taken in the direction of the axis of the microfibril and Y coordinate as the transverse direction. A parametric study was conducted by varying the morphological parameters as follows:

- Long period (L): 86 Å, 91 Å
- Ratio of length of crystallite to amorphous domain ( $l_a/l_c$ ): 0.2, 0.5, 0.75
- Ratio of moduli of crystallite to amorphous domain ( $M_a/M_c$ ): 0.1, 0.13, 0.25

The typical results of stress distribution under bending is shown in Figure 12 in

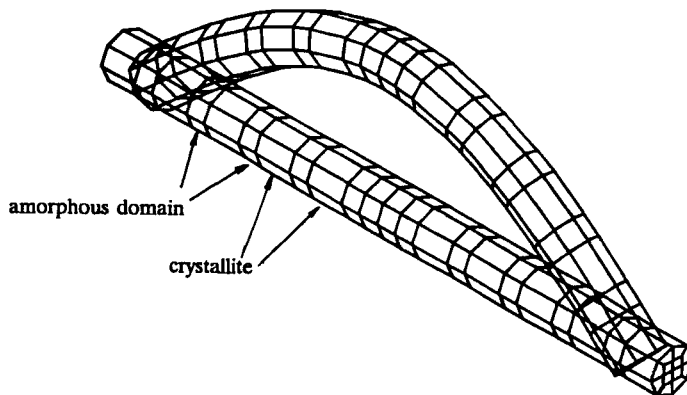


FIGURE 11 Finite element model of microfibril (before and after bending).

TABLE III  
Properties of crystallite and amorphous domain<sup>7,8</sup>

Moduli	Crystallite (GPa)	Amorphous domain (GPa)
E <sub>xx</sub>	25.0	3.26
E <sub>yy</sub>	4.0	2.50
E <sub>zz</sub>	4.0	2.50
G <sub>xy</sub>	1.72	0.93
G <sub>yz</sub>	1.67	0.89
G <sub>zx</sub>	1.72	0.93
Poisson's Ratio		
$\nu_{xy}$	0.16	0.35
$\nu_{yy}$	0.20	0.40
$\nu_{xz}$	0.16	0.35

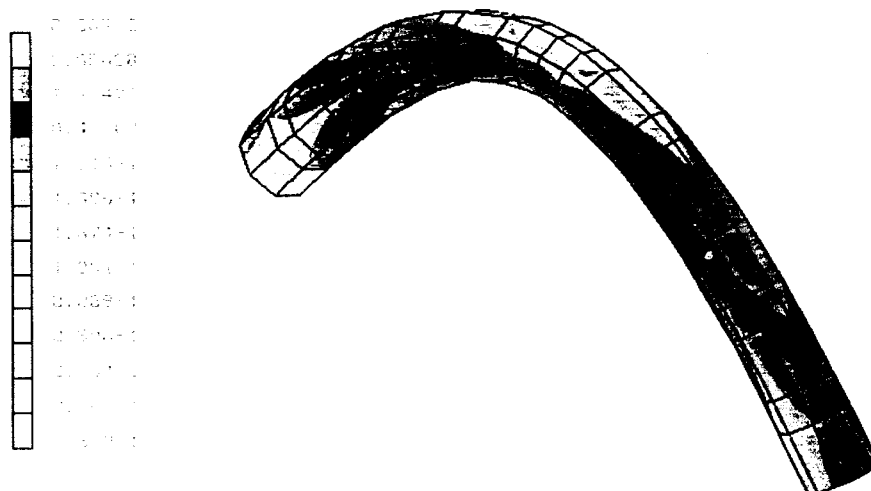


FIGURE 12 Equivalent stress distribution in microfibril under bending.

which equivalent stress contours are plotted. In Figure 13, the effect of the ratio of the length of crystallite to amorphous domain ( $l_a/l_c$ ) on the stress level is plotted using the long period as a parameter. It is seen that as this ratio increases, the stress level decreases but it goes through a minimum. It is worth to note that the minimum occurs at the ratio of actual materials, nylon 6 and nylon 66. It is also seen that a shorter long period (nylon 6) results in lower stress level than the longer long period (nylon 66).

The effect of the long period on stress level is shown in Figure 14 with the ratio of length of the crystallite to amorphous domain ( $l_a/l_c$ ) as a parameter. As the long period increases, the level of the stress increase for all ratios of the crystallite to amorphous domain. Figure 15 shows the effect of the moduli ( $E_{xx}$ ) ratio of amorphous to crystallite domain on the stress level, keeping the modulus of amorphous constant. It is not surprising that as the moduli ratio decreases, i.e., modulus of crystallite decreases, the stress level decreases but a non-linear decrease is seen.

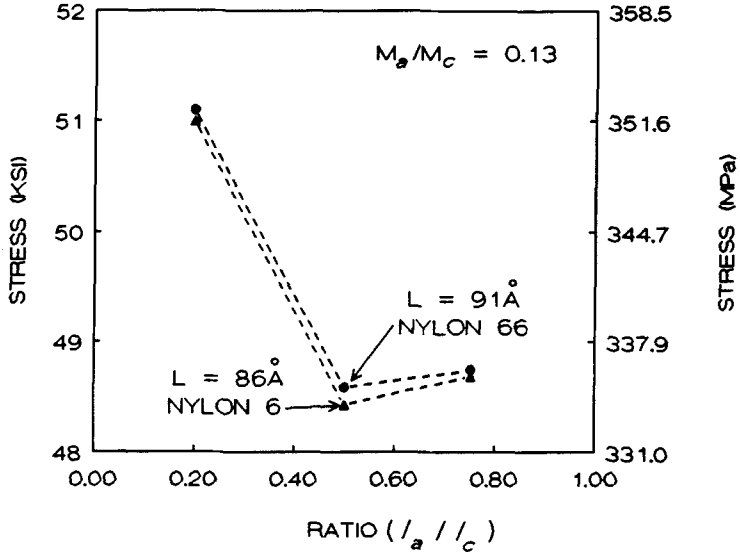


FIGURE 13 Effect of ratio of  $l_a/l_c$  on stress level under bending.

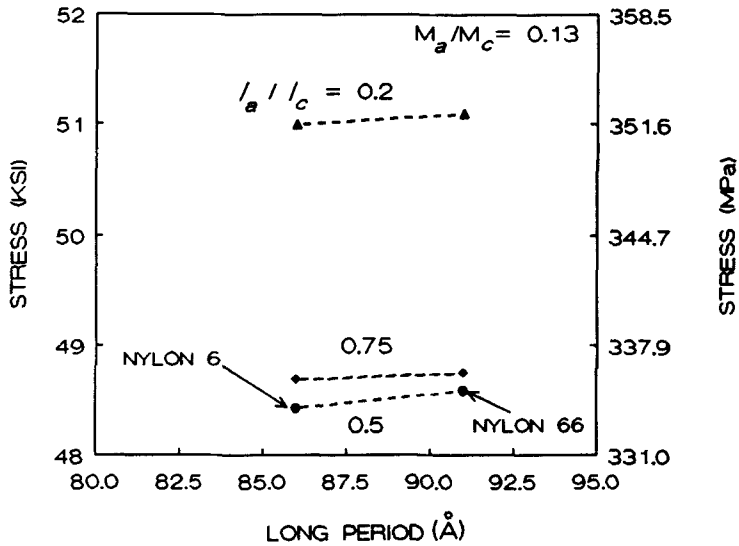


FIGURE 14 Effect of ratio of long period on stress level under bending.

This parametric study clearly shows that nylon 6 has inherent advantageous morphological structure which gives rise to lower stress level than that of nylon 66. The higher damage tolerance and fatigue resistance of nylon 6 are attributable to these morphological differences between nylon 6 and nylon 66. However, this micromechanical analysis does not show the differences between nylon 6 and nylon 66 to the same extent of the differences observed experimentally in fatigue resistance between the two materials. It is therefore concluded that in addition to the micromechanical phenomena, there take place phenomena such as solid state crystalline rearrangements through chain disclination.

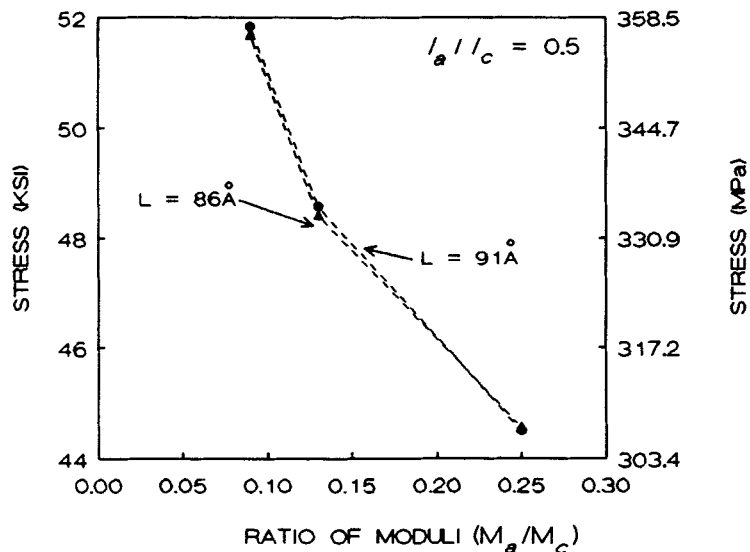


FIGURE 15 Effect of moduli ratio of amorphous to crystalline region on stress level under bending.

## 8. CONCLUSIONS

The morphological analysis showed that the observed performance differences between nylon 6 and nylon 66 fibers on repeated use and especially the outstanding bending fatigue resistance of nylon 6 vs. nylon 66 should be attributed to:

- a. Shorter crystals in nylon 6 fibers
- b. Lower crystalline/amorphous modulus ratio in nylon 6
- c. Large differences in macrolattice perfection (long period distribution) between nylon 6 and nylon 66 with nylon 6 being much more uniform than nylon 66.

To identify the molecular characteristics controlling the crystal dimensions and long period distribution (macrolattice perfection), we considered the heat of fusion and the strain of molecules in the amorphous phase as well as solid state transformation involving motions of disclinations to convert  $\gamma$  crystals into  $\alpha$  crystals and motions of defects to transport the molecule from one crystal to another.

These considerations showed that the critical morphological differences between nylon 6 and nylon 66 fibers have their origins in:

1. The anti-parallel arrangement of molecules in the  $\alpha$  form of nylon 6 crystals (vs. parallel in nylon 66)
2. The shorter repeating unit of nylon 6
3. A shorter distance to reach another low energy position in the lattice of nylon 6 through  $60^\circ$  rotation from  $\alpha$  to  $\gamma$  structure
4. Lower energy in nylon 6 to accommodate crystal defects associated with chain conformation involved in the longitudinal displacement of the molecule.

In summary, the ease of solid state crystalline rearrangements taking place in nylon 6 appears to be the key factor contributing to its impact on bending fatigue

resistance. On the other hand, the same phenomena are responsible for poor dimensional stability (creep), higher cured strength loss during manufacturing of tires, and high shrinkage at elevated temperatures of nylon 6 relative to nylon 66.

**APPENDIX**

**Strain Induced by Rearrangement of Anti-parallel Crystal Structure in Nylon 6**

In forming  $\alpha$  phase crystal structure in which fully extended chains are essentially grouped into hydrogen bonded crystallites, some nylons such as nylon 66 have molecular structure such that hydrogen bonds can be formed without directionality. Other nylons such as nylon 6, in contrast, require that the adjacent molecule must be in opposite direction in order to fully form hydrogen bonds. It is called anti-parallel if the adjacent molecule is in opposite direction, or parallel if the adjacent molecule is in the same direction.

To form anti-parallel crystal structures, molecules are required to switch their positions. This phenomenon is known as disclination shown schematically in Figure 5. In the crystallization process of nylon 6, molecule chains in amorphous domains are strained and twisted in order for the disclination phenomena to take place. In an effort to estimate the degree of strain in the amorphous chains of nylon 6, a simple two dimensional model was used as shown schematically in Figure 16. For simplicity, it was assumed that the chains are straight in the amorphous regions and two possible anti-parallel configurations of nylon 6 were considered.

The degree of strain may be measured by the average length of chains in the amorphous region. The average chain length can be calculated using the assumptions mentioned above. Referring to Figure 16, the average chain length of  $j$ -th chain in the amorphous domain can be expressed as:

$$\bar{C}_j = \frac{1}{n} \sum_{i=1}^n C_{ij} \tag{7}$$

where  $C_{ij}$  is the length of chain bridging  $i$ -th and  $j$ -th chain of the crystalline domains across the amorphous domain, and  $n$  is the number of chains involved.

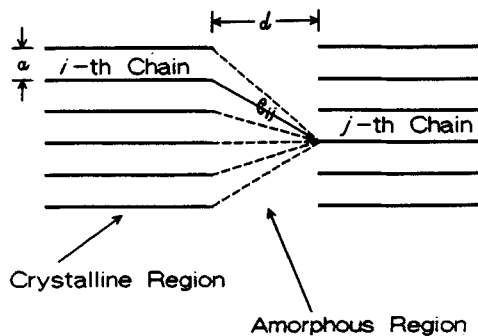


FIGURE 16 Schematic representation of chain length in amorphous region in microfibril.

Thus, for nylon 66

$$\bar{C}_j = \frac{1}{n} \sum_{i=1}^n [d^2 + a^2(j-i)^2]^{1/2} \quad (8)$$

and for nylon 6

$$\bar{C}_j = \frac{1}{n} \sum_{i=1}^n [d^2 + a^2\{j - (2i-1)\}^2]^{1/2} \quad (9)$$

As can be seen from Figure 16, the average chain length  $\bar{C}_j$  varies depending on the location of the chain,  $j$ , thus overall average chain length in an amorphous domain is defined as

$$\bar{C} = \frac{1}{m} \sum_{j=1}^m \bar{C}_j \quad (10)$$

For the case of nylon 6, the chain length depends on the configuration of crystallite (see Figure 17, a and b).

The results of calculation of the chain length in the amorphous regions are shown in Table IV in terms of the number of chains involved and  $\alpha$  crystal configurations. As seen from this table, the average chain length of nylon 6 is longer than that of

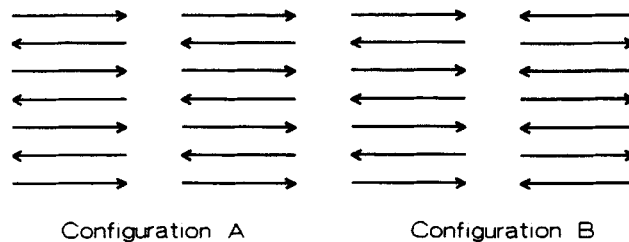


FIGURE 17 Anti-parallel configurations of nylon 6 crystals.

TABLE IV  
Average chain length of amorphous phase (Unit: Å)

Number of chains	Nylon 66	Nylon 6 (Configuration A)	Nylon 6 (Configuration B)
2	30.954	31.281	31.268
3	31.980	32.522	32.259
4	33.312	33.617	33.699
5	34.891	35.297	35.171
6	36.668	36.950	36.945
7	38.606	38.947	38.870
8	40.674	40.935	40.932
9	42.849	43.150	43.097
10	45.111	45.358	45.355

nylon 66 and thus higher strains are expected to develop. Since the average chain length in the amorphous regions is longer, the crystallite length is shorter for nylon 6 than for nylon 66.

The strain energy of a chain to form an anti-parallel  $\alpha$  crystal was estimated by idealizing the motion of disclination as schematically shown in Figure 18. The strain energy increase,  $\epsilon_s$ , can be defined as

$$\epsilon_s = \int F \cdot D(x) dx \tag{11}$$

where  $F$  is the force required to move a chain per unit length of chain and  $D(x)$  is the distance of chain movement due to disclination. Therefore, the strain energy increase is proportional to the shaded area shown in Figure 18.

The strain energy increase due to the disclination is then calculated, i.e.,

$$\Delta\epsilon_s = \frac{1}{2} F \{ 2al_c + l_a(a + \Delta l \tan \theta) \} \tag{12}$$

where  $\theta$  is the angle of the chain in the amorphous domain before the disclination. Assuming that the maximum value of  $\theta$  is to be  $45^\circ$ , Equation 12 becomes

$$\Delta\epsilon_s = \frac{1}{2} F \{ 2al_c + al_a \} \quad \text{when } \theta = 0^\circ \tag{13}$$

and

$$\Delta\epsilon_s = \frac{1}{2} F \{ 2al_c + l_a(a + \Delta l) \} \quad \text{when } \theta = 45^\circ \tag{14}$$

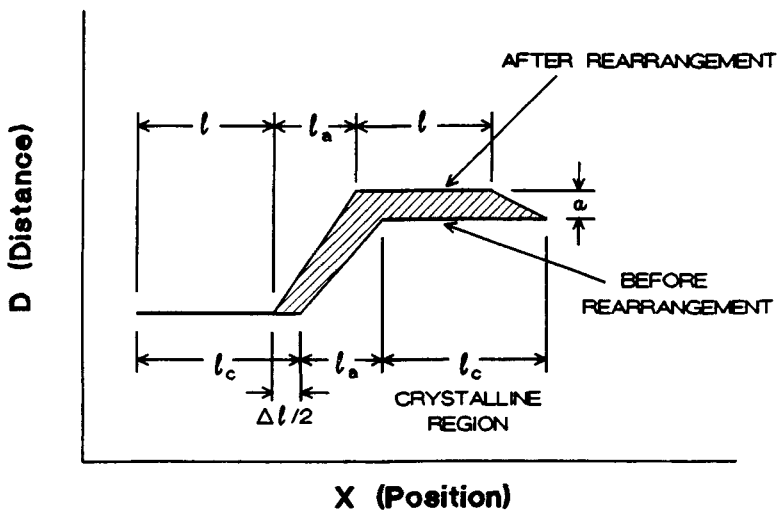


FIGURE 18 Disclination of chain to form anti-parallel configuration.



where  $l_c$  is the length of crystallite and  $l_a$  is the length of amorphous domain.  $\Delta l$  is the increase in chain length in amorphous domains due to the disclination and its magnitude is shown in Table IV. The average value of the strain energy increase may be represented by averaging Equations 13 and 14, yielding,

$$\Delta \epsilon_{avg} = \frac{1}{2} F \left\{ 2al_c + l_a \left( a + \frac{\Delta l}{2} \right) \right\} \quad (15)$$

In a similar manner, the average energy level of the chain before disclination can be derived by choosing the energy level of straight chain as a reference energy level:

$$\epsilon_{avg} = \frac{1}{2} F \left( l_c l_a + \frac{l_a^2}{2} \right) \quad (16)$$

It is seen from Equations 15 and 16 that the increase in strain energy due to disclination is approximately 14% of the energy level before disclination, when

$$l_c = 60 \text{ \AA}$$

$$l_a = 30 \text{ \AA}$$

$$\Delta l = 0.3 \text{ \AA}$$

$$a = 5 \text{ \AA}$$

This implies that the heat of fusion of nylon 6 is approximately 16% lower than that of nylon 66. Actual experimental data show that the heat of fusion of nylon 6 is 9.4% lower than that of nylon 66 (see Table I). Note that the above derivation is an approximation for idealized situation, therefore, some discrepancy is expected.

## References

1. D. C. Prevorsek, S. Murthy and Y. D. Kwon, *Rubber Chem. Tech.*, **60**, 659 (1987).
2. K. Schneider and K. Wolf, *Kolloid Z.*, **134**, 149 (1953).
3. D. C. Prevorsek, Y. D. Kwon and R. K. Sharma, *J. Mat. Sci.*, **12**, 2310 (1977).
4. Y. P. Khanna, *Polymer Engineering Science*, **30**(24), 1615 (1990).
5. O. C. Zienkiewicz, "The finite element method," McGraw-Hill Book Co., (1977).
6. Marc User Manual, Vol. A, B and C. Marc Analysis Research Corporation.
7. I. M. Ward, "Structure and Properties of Oriented Polymers," Chapter 7.242, John-Wiley (1975).
8. T. W. Clyne, *J. Mat. Sci. Letters*, **9**, 336 (1990).
9. D. C. Prevorsek, H. B. Chin and Y. D. Kwon, *Int. J. Polym. Materials* (article in press).